Article

Optimal Planning and Deployment of Hybrid Renewable Energy to Rural Healthcare Facilities in Nigeria

Lanre Olatomiwa [1,2,*], Omowunmi Mary Longe [2], Toyeeb Adekunle Abd'Azeez [1], James Garba Ambafi [1], Kufre Esenowo Jack [3] and Ahmad Abubakar Sadiq [1]

[1] Department of Electrical & Electronics Engineering, Federal University of Technology, Minna P.M.B 65, Niger State, Nigeria; ambafi@futminna.edu.ng (J.G.A.); ahmad.abubakar@futminna.edu.ng (A.A.S.)

[2] Department of Electrical & Electronic Engineering Science, University of Johannesburg, Johannesburg 2006, South Africa; omowunmil@uj.ac.za

[3] Department of Mechatronics Engineering, Federal University of Technology, Minna P.M.B 65, Niger State, Nigeria

* Correspondence: olatomiwa.l@futminna.edu.ng; Tel.: +234-906-161-1760

Abstract: This paper takes a cursory look at the problem of inadequate power supply in the rural healthcare centres of a developing country, specifically Nigeria, and proffers strategies to address this issue through the design of hybrid renewable energy systems combined with the existing unreliable grid in order to meet the healthcare load demand, thus ensuring higher reliability of available energy sources. The simulations, analysis and results presented in this paper are based on meteorological data and the load profiles of six selected locations in Nigeria, using which hybrid grid-connected systems integrating diesel, solar and wind energy sources are designed with configurations to give optimum output. The optimised design configurations in the considered case study, Ejioku, Okuru-Ama, Damare-Polo, Agbalaenyi, Kadassaka and Doso, produce very low energy costs of of 0.0791 \$/kWh, 0.115 \$/kWh, 0.0874 \$/kWh, 0.0754 \$/kWh, 0.0667 \$/kWh and 0.0588 \$/kWh, respectively, leveraging solar and wind energy sources which make higher percentage contributions at all sites. The load-following-dispatch strategy is adopted at all sites, ensuring that at every point in time, there is sufficient power to meet the needs of the healthcare centres. Further works on this topic could consider other strategies to optimise general energy usage on the demand side.

Keywords: renewable energy; hybrid energy optimization; rural electrification; renewable energy penetration

1. Introduction

The global population, industrial and commercial activities, technological innovations such as electric vehicles, robust base transmission systems (BTS), smart cities, and many other aspects of human existence are experiencing an exponential increase, which has resulted in very high energy demands and consumption [1]. This calls for a massive increase in the available global energy resources to meet the increasing demand and avoid energy deficits. The minimum expected electrical energy per year in countries is 250 kilowatt hours (kWh) for a rural household and 500 kWh for an urban household [2], as recommended by the International Energy Agency (IEA). However, Moss et al. [3] reviewed these data and proposed a minimum of 1000 kWh per person per year to fully achieve the aim of Sustainable Development Goal 7 (SDG7): "Ensuring access to affordable, reliable, sustainable and modern energy for all" [4]. Many countries are still in a deficit of electrical energy supply needed to meet the demands of their population, having as little as 137.53 kWh per capita per year, resulting in as little as 15.6 kW available per head in 2021 [5]. This low energy output thus has a very high negative impact on healthcare facilities,

especially those in rural settlements [6]. In order to meet SDG7 by 2030, significant and purposeful efforts need to be directed towards providing electrical energy to rural areas, as most people without access to electricity reside in these areas [7].

Generally, while urban settlements receive better preferential treatment regarding resource allocation, rural areas do not benefit much from resource allocation. Often, the resulting shares allocated to these rural areas are insufficient to supply the population [8]. Accessibility to good healthcare services in rural areas is greatly impeded by the unavailability/insufficiency of the electrical energy supply to these healthcare centres. This results in the poor health status of the people in the area, a high mortality rate, a high density of people with terminal diseases, and an overall decline in the living conditions of the populace [9]. Thus, there is a need for scalable and sustainable solutions to help curb these issues and provide good healthcare services.

Many healthcare centres in Nigeria are suffering from an electricity supply shortage due to the unreliability of the public utility system; moreover, many areas do not have access or are not connected to the public utility (national grid). It is this premise that motivates this research. The current situation is characterised by diesel-powered generators generically being employed in standalone and off-grid generating systems for most rural healthcare centres. In view of the high cost of fuel and carbon emissions, which are detrimental to the environment, this solution alone is termed inefficient [9,10]. Over the years, researchers have not ceased efforts to ensure that alternate sources of energy, particularly renewables, are deployed to provide energy solutions in our economy today to help mitigate energy security issues, thus giving rise to the integration of these alternative energy sources [11]. Renewable energy systems are considered a necessity for rural healthcare facilities' operational efficiency; most of these remote health centres are located where the grid system cannot be accessed, thus hampering the operation of primary health services in rural areas [6].

Numerous energy access and quality issues exist in developing and undeveloped nations, endangering the lives of patients, healthcare staff, and infrastructure. Even with diesel or petrol, grid electricity proves challenging to maintain, and rural health clinics need help to solve this problem. Since most developing nations live in rural or isolated places, it is imperative to subscribe to renewable systems such as solar energy in hospital operations [12]. Rural communities can likely boost local economic activity by producing renewable energy plants for various uses, including the primary healthcare sector. Access to energy for healthcare is essential to innovate and deliver a sizable number of stable healthcare practices, among other business outlooks [13]. Integrating renewable and non-renewable energy sources proves more economically friendly, improves environmental friendliness, and is considered durable compared to traditional systems of single-generation sources [14].

Achieving an optimised configuration of energy resources for a given demand load centre given the available energy resources, reducing the cost of energy, carbon emissions, and fuel costs and meeting the hourly energy demands requires the adoption of proper strategies governing the dispatch sent and energy allocation [10]. These dispatch strategies are rules and algorithms governing the energy flow in hybrid systems [15].

2. Literature Review

Many studies have looked into the unreliability of electrical energy supply to consumers, and have proffered technical and economical solutions. Most of these studies used HOMER software to solve optimisation problems, as revealed by Sminha and Chandel [16]. Most projects and research on rural electrification have focused on solving electricity problems using standalone systems. Abnavi, M.D. et al. [17] showed that standalone systems based on the use of diesel generators could greatly reduce the cost of energy, but the economics of such systems are greatly affected by and dependent on the cost of fuel. A study was conducted by Shezan, S.A. et al. [18] to find the best dispatch strategy, considering a techno-economic and system stability analysis with optimal sizing for two

locations in Bangladesh. A study was carried out on the impact of energy dispatch strategies on the design optimisation of hybrid renewable energy systems [10], and a techno-economic feasibility and sensitivity analysis of the off-grid hybrid renewable energy system was performed in order to find the electric load requirements of an unelectrified rural village in Chamarajanagar district, Karnataka (India) [19].

In [20], the authors emphasise that renewable energy solutions are appropriate for on-grid and off-grid applications, acting as a supporter for the utility network or rural location, and went ahead also to examine hybrid renewable energy power production systems with a focus on energy sustainability, reliability due to irregularities, techno-economic feasibility, and environmentally friendliness. At the same time, a techno-economic analysis of renewable energy-based micro-grids (MG) considering incentive policies was presented in [21] for developing countries such as Iran. The developed framework for the optimal planning of a renewable energy-based MG considering incentive policies indicates that the proposed incentive policies reduce the MG's total net present cost (NPC) and the amount of carbon dioxide (CO_2) emissions.

A comparison study of HRES for the electrification of a rural city in Algeria was carried out wherein a PV/wind/battery/electrolyzer/H2 tank/fuel cell hybrid system was proposed as the most optimal solution [22]. Another study was conducted to find a technically feasible and economically viable hybrid energy solution for off-grid electrification for the village of Korkadu in the Puducherry region in India, in order to provide the least costly configuration of solar PV, wind turbines, bio generators, and battery bank backup to meet the projected demand [23]. M. Krishnamoorthy [24] performed a feasibility design and techno-economic analysis of a hybrid renewable energy system for the rural electrification of a remote village, Korkadu, located in the Union Territory of Pondicherry, India, as a case study using HOMER software and a combined dispatch strategy.

A hybrid off-grid renewable power system has been proposed for sustainable rural electrification in Benin, Nigeria; the proposed system uses PV/DG/battery configurations to provide power for rural areas [25]. A case study on a demand side management-based cost-optimised battery-integrated hybrid renewable energy system for remote rural electrification was carried out by Dhavala, R.K. et al. [26], and leveraged an HRES configuration involving PV, wind turbines, diesel generators and batteries, while incorporating extra optimisation at the consumer end using demand side management. Another hybrid grid-tie electrification analysis of bio-shared renewable energy systems for domestic application was presented in [27], taking Gaza as a case study.

A comprehensive study on the optimal planning and design of hybrid renewable energy systems for microgrid (MG) applications at Oakland University, using HOMER Pro for a performance analysis of the technical, economic, and environmental aspects of integrating renewable energy technologies, is presented in [28]. The work addresses the unmet load in the MG system design to ensure the university's electricity demand is consistently met. On the other hand, the high fluctuation in PV sources makes it difficult to accurately predict short-term PV output power generation, leading to ineffective system planning and effects on energy security. Khortsriwong, N. et al. [29] presented several well-known deep learning techniques to forecast short-term PV power generation in a real-site floating PV power plant of 1.5 MWp capacity at Suranaree University of Technology Hospital, Thailand.

Some issues, such as the uncertainty of renewable resources, characterise sizing methodologies for the HRES. Thus, Medina-Santana and Cárdenas-Barrón [30] proposed a sizing methodology that includes long short-term memory (LSTM) cells to predict weather conditions in the long term, multivariate clustering to generate different weather scenarios, and a nonlinear mathematical formulation to find the optimal sizing of an HRES.

Most of the cited literature in this work clearly and sufficiently solves the issues presented using HOMER Pro software. Various dispatch strategies and configurations that are fitting for the available resources in the areas under review have been presented;

however, their simulations and design considerations do not make provisions for grid-connected systems [10,17–26], while generically referring to the load demand and profile of the entire rural area as a case study. However, Al-Najjar, H et al. [27] presented a design that considered this observation in the present paper; there is an observable gap in the techno-economic analysis, as the techno-economic data for the grid utility was not completely incorporated into the simulation analysis presented. Although ref. [26] adopts extra optimisation on the demand side, the system is not grid-tied with a generic rural area load.

This paper, therefore, contributes to existing knowledge by addressing the setbacks identified in the cited related literature in the following ways.

- We design an optimum grid-tied energy system configuration to suffice for the energy requirements of some specific rural healthcare centres in Nigeria.
- We adopt LF dispatch strategies to account for the deficiency of energy supplied, while ensuring optimal system operations and reductions in energy wasted.
- The developed optimum grid-tied configuration and the adopted dispatch strategies contribute to an overall reduction in emissions.
- We make an initial attempt to integrate the HRES into the national grid through healthcare centres in Nigeria.

Essentially, the provisions in the configurations presented in this research are grid-tied. This shows that despite the unreliability of the public utility in some areas, there is little time when grid power can be leveraged. The HRES is integrated into the national grid, and this study presents the percentage contribution and penetration of the HRES in the overall system.

In addition to the design of grid-tied configurations, the results presented in this paper were simulated with HOMER using actual data for the hourly load demand and consumption of the various healthcare centres as input parameters for the load profiles. This goes a long way toward making the results practical and adaptable in their implementation. The results will provide necessary and useful data for further research and project implementation in the electrification of these rural healthcare centres.

3. Methodology

The methodological approach utilised in this research involves data collection, preparation, assessment and validation, simulation, and results. The gathered data are from rural public healthcare centres (PHCs) in six different locations in Nigeria, which are independent. The geographical information of these PHCs is presented in Section 3.1 of this paper.

A number of data types are collected and used to achieve the desired results in this study. One is the real-time load consumption and demand of the PHC, as shown in Section 3.4.1. Also, the situational reports on the reliability and availability of the utility or grid are collected and discussed in Section 3.4.2. Wind and solar data are sourced and collected from the Nigeria Meteorological Agency (NIMET). These recent and accurate data will give proper insight into these areas' available renewable energy resources. These collected data are prepared and processed into a suitable format, making the data ready for simulation in HOMER Pro. The results obtained are presented and discussed in Section 4 of this paper.

3.1. Geographical Data of Selected Locations

In a bid to develop reliable and useful data, the selected locations in this work are widely dispersed, covering the six geopolitical zones in Nigeria, as illustrated in Figure 1. Table 1 presents a general overview of the geographical information about the PHC's location. This approach will give a broader insight into how system configurations and optimal solutions for HRES are affected by the locations and their performance in separate regions of Nigeria. In order to explicate and fully grasp how and why the separate regions

will have entirely different configurations irrespective of their separate load profiles, information about the meteorological data is presented in this section [9]. While the North-west (NW) and North-east (NE) zones have a hot, semi-arid climate type, the North-central (NC) region is tropical. Tropical and dry regions are associated with high temperatures. These differences, among others, alter the design parameters in determining the optimum solutions for these areas.
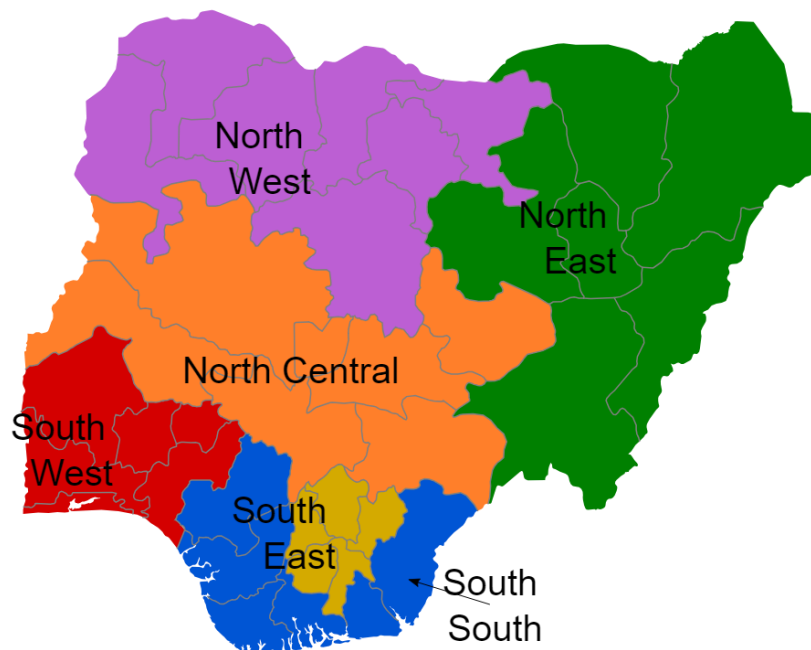

Figure 1. Map of Nigeria showing different geopolitical zones.

Table 1. Geographic information of the selected locations.

Location	State	Zone	Latitude (°N)	Longitude (°E)	Altitude (Meters)	Climate Type
Ejioku	Oyo	South-west (SW)	7.475	4.071	330	Tropical wet monsoon
Kadassaka	Sokoto	North-west (NW)	13.68	5°31′59″	220	Hot semi-arid
Damare Polo	Adamawa	North-east (NE)	9°12′48″	12°29′23″	353.8	Hot semi-arid
Doso	Plateau	North-central (NC)	9.154	9.713	1217	Tropical
Agbalaenyi	Enugu	South-east (SE)	6.265	7.281	247	Humid
Okuru-Ama	Rivers	South-south (SS)	4°48′59″	7°3′3″	465	Monsoon

3.2. Renewable Energy Resource Assessment

Renewable energy resources determine the extent of renewable energy penetration in power generation in a particular location. These sources include solar, wind, biomass, hydro, and others. However, sun and wind energy are the most abundant and readily available for utilisation [9]. Therefore, a proper investigation must be conducted to determine which combination of resources is most feasible for power generation at a selected site. Assessment of renewable energy resources requires a good amount of data for the accuracy of the analysis. The geographical data of the location under study and the metrological data (solar GHI and wind speed) are the basic data inputs for the simulation.

The software calculates the possible power output that can be achieved from the resources based on the solar and wind speed data provided. The solar and wind data of the six stations are analysed in Sections 3.2.1 and 3.2.2, respectively. Since the locations have different climatic statuses, variation is expected in their penetration levels. The average daily solar radiation data from 4 to 16 years was prepared monthly for better accuracy.

3.2.1. Solar Global Horizontal Irradiance (GHI)

As earlier established, the solar GHI data are obtained from NIMET. Global horizontal irradiance (GHI) is the total solar radiation incident on a horizontal surface. It is the sum of direct normal irradiance (DNI), diffuse horizontal irradiance, and ground-reflected radiation [31]. It is given in kWh/m²/day. HOMER uses Solar GHI to compute flat-panel PV output, while computing the effects using the Hay and Davies, Klucher and Reindl (HDKR) model according to Equation (1):

$$\bar{G}_T = (\bar{G}_b + \bar{G}_d A_i)R_b + \bar{G}_d(1 - A_i)\left(\frac{1+\cos\beta}{2}\right)\left[1 + \mathcal{F}\sin^3\left(\frac{\beta}{2}\right)\right] + \bar{G}\rho_g\left(\frac{1-\cos\beta}{2}\right) \tag{1}$$

where

β = the slope of the surface [°];
ρ_g = the ground reflectance, which is also called the albedo [%];
$\bar{G}_b$ = the beam radiation [kW/m²];
$\bar{G}_d$ = the diffuse radiation [kW/m²];
R_b = the ratio of beam radiation on the tilted surface to beam radiation on the horizontal;
A_i = measure of the atmospheric transmittance of beam radiation.

A pictorial comparative analysis of the GHI of each location is shown in Figure 2. The inputs are the average monthly GHI from 5 to 16 years. It is observed that Doso and Damare-polo, which are, respectively, located in the tropical and hot–semi-arid regional parts of Nigeria, have the highest solar penetration. However, the stations located in the southern part, which include Okuru-ama, Ejioku, and Agbalaenyi, exhibit lower solar potential.
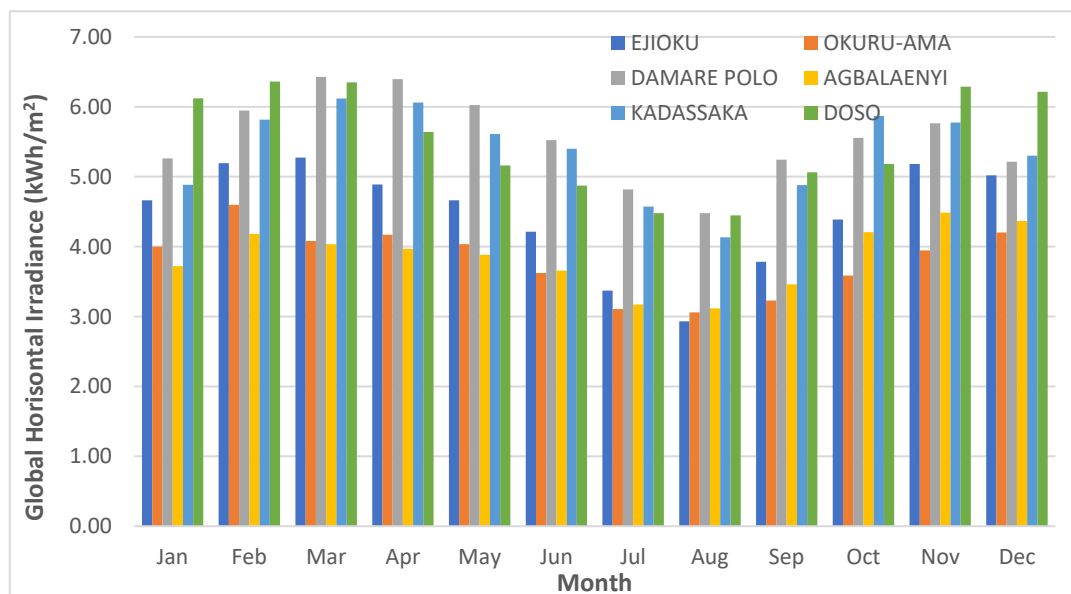

Figure 2. Average solar data of selected locations.

3.2.2. Wind Speed Data

As previously stated, the wind speed data are obtained from NIMET and given in m/s. These data forms the basis from which the best wind turbine configuration is developed to take advantage of the existing wind speed conditions in the locations, as the analysis of the wind energy potential is based on wind speed data. However, it is important to take into account the fact that there is variability in wind speed with respect to height (in this case, the height of the turbine) [32]. To account for this, HOMER uses the logarithmic profile (or log law), which assumes that the wind speed is proportional to the logarithm of the height above ground [33], as shown in Equation (2).

$$\frac{U_{hub}}{U_{anem}} = \frac{\ln(Z_{hub}/Z_o)}{\ln(Z_{anem}/Z_o)} \tag{2}$$

where

U_{anem} = the wind speed at anemometer height [m/s];

U_{hub} = the wind speed at the hub height of the wind turbine [m/s];

z_{hub} = the hub height of the wind turbine [m];

z_{anem} = the anemometer height [m];

z_o = the surface roughness length [m].

A comparative analysis of wind speed is presented in Figure 3. From this figure, the data show that the Northern region locations, Doso (Northcentral), Kadassaka (Northwest), and Damare-polo (Northeast), have the highest wind penetration level, followed by Agbalaenyi (Southsouth), with the lowest potential stations at Ejioku (Southwest) and Okuru-ama (Southeast); Doso has the highest level overall. Additionally, it can be observed that there is a relative drop in wind speed in centres starting from May to September, after which there is an observed rise in relative wind speed.
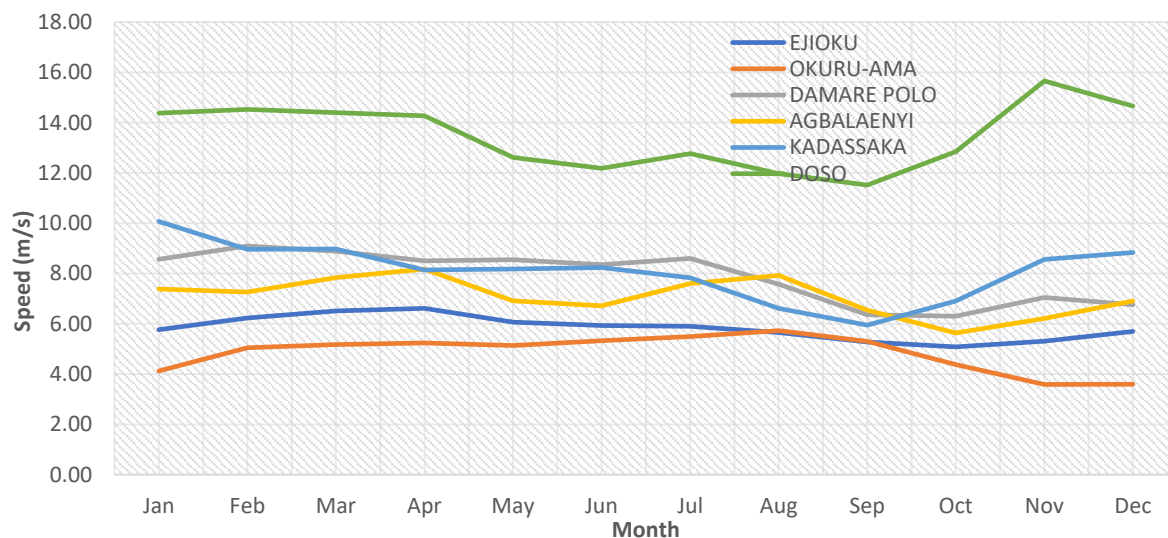

Figure 3. Wind speed of the selected locations.

3.3. Energy Needs Assessment of PHC in the Selected Sites

An effective assessment of energy demand is one of the prerequisites to ensure the proper selection of a suitable system combination. A load analysis of the equipment used in healthcare facilities is required to plan and design the energy system. With this step, we can easily obtain the total connected load, average load, peak demand, and hourly power usage throughout the 24 h.

This section gives the load descriptions for the six stations. These include the equipment power rating, hourly demand, and total energy demand. A proper description of the site's load is provided in Appendix A, Tables A1 and A2, as collected on site. From the data collected through site visits, load analyses, and questionnaires, it is observed that all six healthcare centres are faced with the problem of unreliable grid supply. The grid's unreliability results from very old electricity transmission equipment and materials, improper load shedding, and sometimes unplanned and unscheduled downtime. This poses problems for healthcare centres as electrical energy is needed to power the medical equipment. According to information gathered from the sites, there is an average availability of electrical supply of about 10% to 15% per year. This equals about 876 h of electrical energy

supply per year, compared to 8760 h/yr. With this problem comes the need for a reliable system.

As a result of the unreliable supply of public utilities, all the healthcare centres have resorted to using diesel generators to meet their demands. This, in turn, is very costly, as the cost of energy is very high considering the cost of diesel; further, the running hours of the diesel generator sum up to no less than 14 h daily on average for the various healthcare centres, totalling no less than 5000 h per year (about 60%).

Loads in the health centres are a combination of heavy and light loads. Light loads or small energy-consuming appliances are lighting, fans, televisions, and other miscellaneous devices or loads. Some medical equipment includes a centrifuge, an electrical microscope, sterilisers, an X-ray machine, a haematology analyser, a blood chemical analyser, and a few others.

The approximate daily watt hour load demands of the healthcare centres are 67.306 kWh/d, 50.757 kWh/d, 49.739 kWh/d, 34.176 kWh/d, 23.916 kWh/d and 30.65 kWh/d for Doso, Agbalaenyi, Okuru-Ama, Ejioku, Kadasaka, and Damare Polo, respectively. These centres are open 24 h a day, and at every point in time, loads are consumed by the centres. These data form part of the input data for the HOMER simulation.

The situational report shows that the available energy supply is deficient, and the diesel generator is not cost-effective. Hence, there is a need for a more scalable and reliable configuration to be adopted to improve the efficiency of these PHCs.

3.4. Homer Software Description and Input Data

HOMER (Hybrid Optimization for Multiple Energy Resources) is a piece of software invented by the National Renewable Energy Laboratory (NREL) for the simulation, optimisation, and sensitivity analysis of renewable energy systems [34]. HOMER software is designed to provide an optimised system configuration by evaluating the available technology options based on their energy resource potential in the target location [35]. The HOMER methodology employed in this case study is presented in Figure 4 [36].
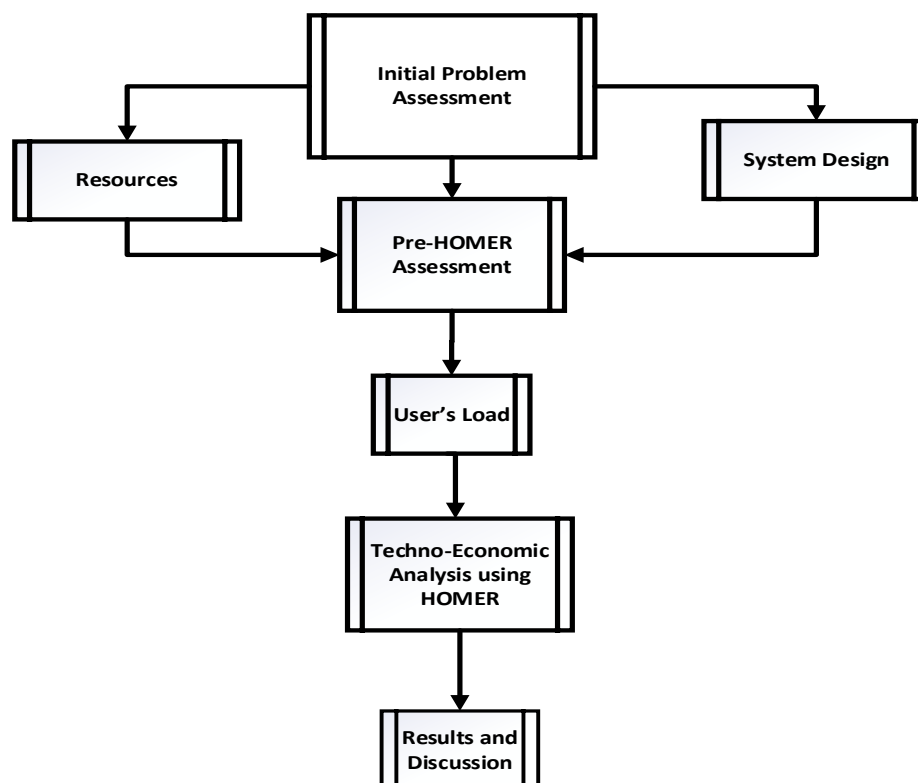

Figure 4. HOMER methodology.

The data used in the simulation in HOMER Pro software include load profile data, wind speed, diesel fuel consumption, and a model of an unreliable grid and global horizontal irradiance (Solar GHI) for PV analysis.

3.4.1. Load Profile

The load profile forms the basis for the configurations and solutions. The load profile of each health centre is taken over 24 h. The load demand differs for each selected location, with Doso peaking at the highest value of 6.827 kW. A comparative analysis of the load profiles of the healthcare centres distributed over 24 h is presented in Figure 5.
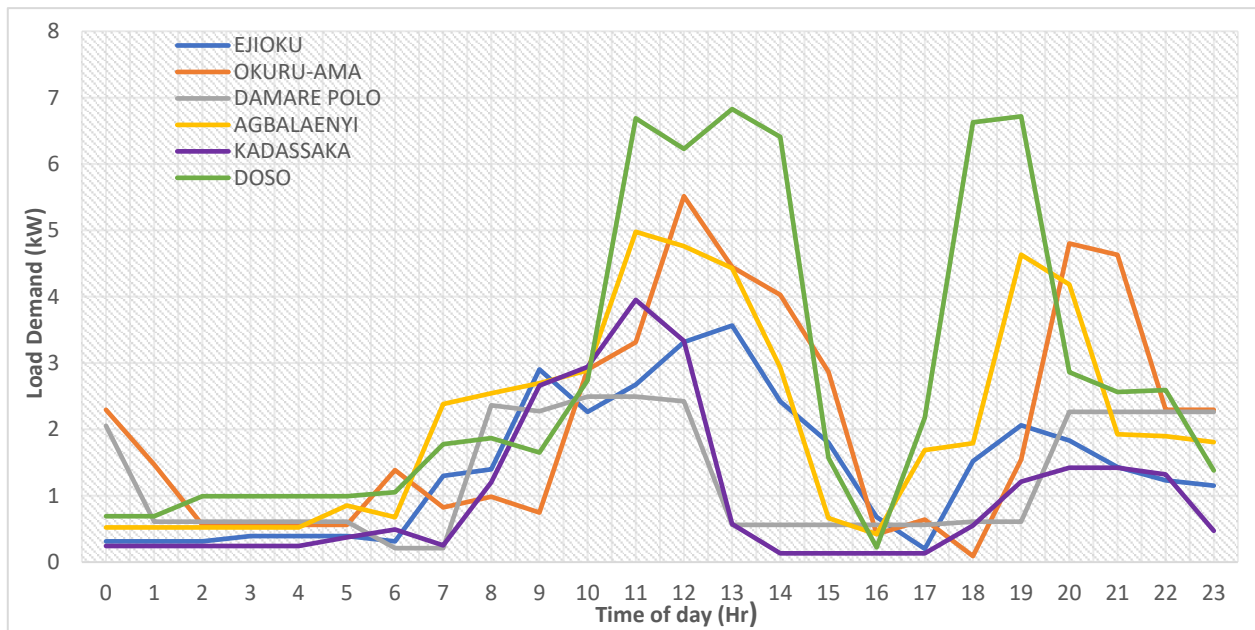

Figure 5. Comparative analysis of sites' load profiles.

As observed in the load distribution, the system does not utilise all the equipment at every instance during the day; the optimisation begins at the consumer end. From the data presented in the chart above, it can be observed that Doso Healthcare Center has the highest peak load of about 6.827 kW, occurring between 11:00 a.m. and 2:00 p.m. during the day, when there is a peak in load consumption. Conversely, Damare Polo and Kadassaka have the lowest average daily load consumption. The daily load profiles for various sites that serve as input to the HOMER software are shown in Figure 6. It can be deduced that there is more demand for power during the day than at night. The maximum demand of each station was set to 10% day-to-day random variability and a 15% timestep. This redefines the peak load of the station for better accuracy of results. The need to redefine peak load arises from the variability in daily energy demand, which is influenced by consumers' usage patterns and connected loads. Adapting the definition of peak load to reflect these changing requirements for effective energy management is important. These details will help to a great extent to determine the nature and size of the hybrid system configuration.
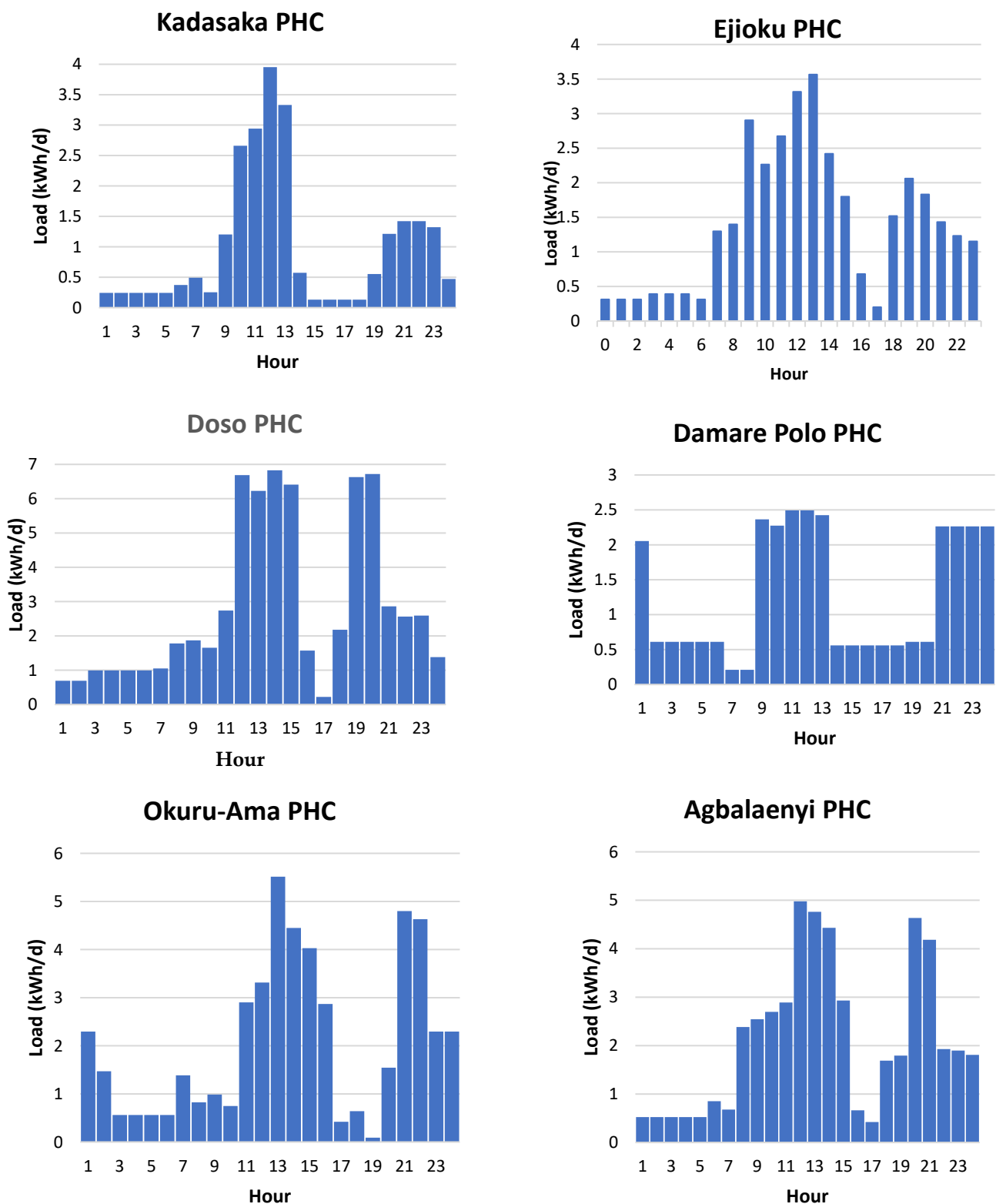
Kadasaka PHC

Ejioku PHC

Doso PHC

Damare Polo PHC

Okuru-Ama PHC

Agbalaenyi PHC

Figure 6. Load profiles input data for various sites.

3.4.2. Grid Supply

As mentioned earlier, the current condition of the supply in all the considered PHCs is an unreliable grid, which is as low as 30% in some centres. A model of a randomly generated profile for outages and normal operation of the grid is generated and provided

as input data for the grid system to obtain the optimal solution from a grid-tied system. However, to do this, the grid's outages and normal operating conditions are arbitrarily selected from a 365-day profile. This selection, though arbitrary, is constrained to a maximum of 30% of normal operation, that is, when there is a power supply in the PHC.

From the above, a more randomised grid profile is generated by constraining the mean outage frequency to 100/yr, with a mean repair time of 3 h and repair time variability of 0%. The grid model produced from the profile is shown in Figure 7, and the constraint parameters presented here are shown in Figure 8. The purpose of this model is to simulate how the grid operates in selected locations. In the model, the green area represents normal operation when there is a power supply, while the black section signifies periods of outage. The data generated by this model are used as input for simulations, allowing the software to better understand the grid's status in these locations. This forms the basis for the unreliable grid input in the research work. Additionally, to obtain a more insightful result, the model is generated differently for each of the PHCs. It is noteworthy that the designed grid parameters do not allow sales of excess available energy in the centres to be sold back to the grid. Hence, the grid export energy tariff is capped at 0 $/kWh.
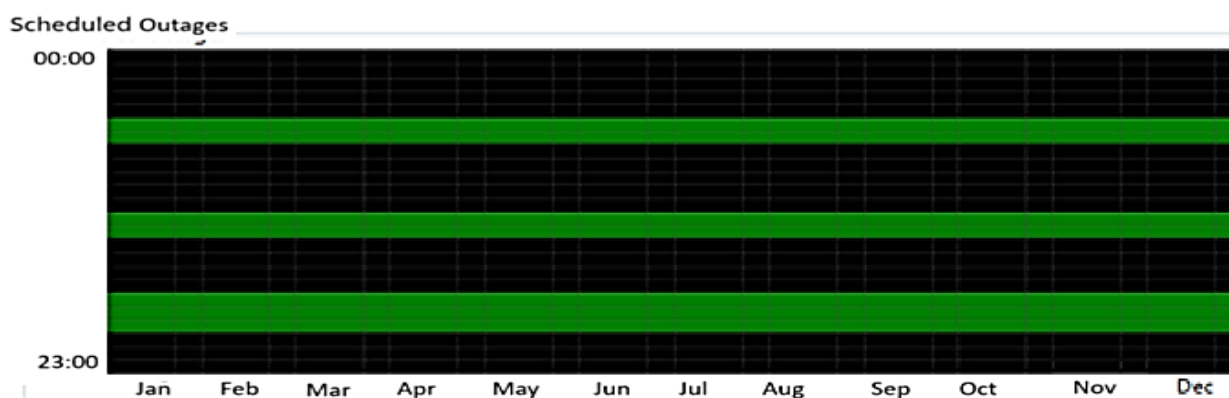

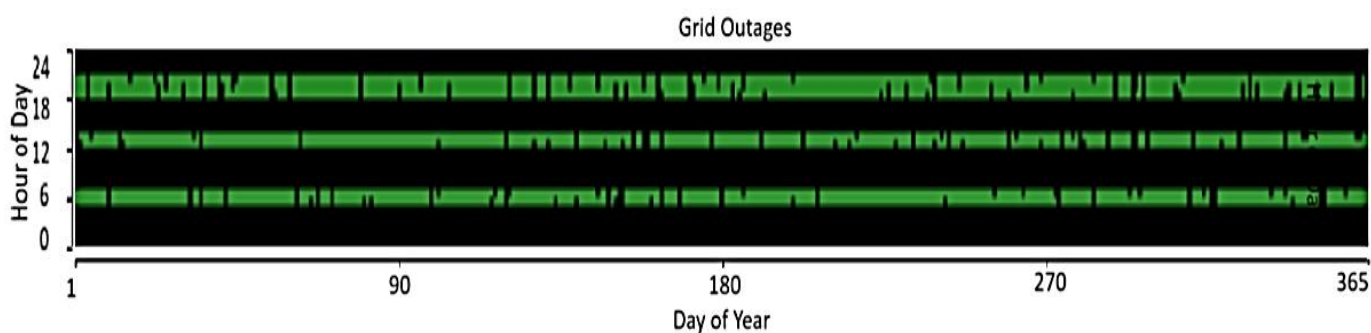**Figure 7.** Profile of arbitrarily selected outage.

Figure 8. Model of unreliable grid input.

3.4.3. Techno-Economic Data and Specifications

Table 2 summarises the techno-economic data and specifications used in this study. The prices and parameters detailed here are based on recent data from Ngpricehunter websites and distribution companies' tariff rates [37,38]. The data presented in this section greatly affect the overall system cost, particularly the inflation rates, as the project's lifespan is 25 years. The annual capacity shortage is set to zero. This ensures an energy supply to the PHCs at every point in time, thus justifying the reliability prospects presented in the design configurations.

The system's life-cycle cost is represented by the total net present cost (NPC). The NPC is a composite of the system component's initial capital costs, replacement costs,

annual operating and maintenance costs, and fuel costs, and is computed using Equation (3) [9,39].

$$NPC_{Tot} = \frac{C_{ann,Tot}}{CRF} \tag{3}$$

where CRF is the capital recovery factor and can be evaluated in terms of interest rate (i) and project lifetime (n), as

$$CFR = \frac{i(1+i)^n}{(1+i)^n - 1} \tag{4}$$

However, in a PV/wind/diesel/battery hybrid system, the total annualised cost of the entire hybrid system can be represented as

$$C_{ann,Tot} = \sum_{N=1}^{N_{pv}} C_{ann,pv} + \sum_{N=1}^{N_{wt}} C_{ann,wt} + \sum_{N=1}^{N_{batt}} C_{ann,DG} + \sum_{N=1}^{N_{batt}} C_{ann,bat} + \sum_{N=1}^{N_{conv}} C_{ann,conv} \tag{5}$$

where N_{pv}, N_{wt}, N_{DG}, N_{bat}, and N_{conv} are numbers of PV modules, wind turbines, diesel generators, batteries and converters, respectively. $C_{ann,pv}$, $C_{ann,wt}$, $C_{ann,DG}$, $C_{ann,bat}$ and $C_{ann,conv}$ are total annualised costs for each component (PV modules, wind turbine, diesel generator battery and converter) as computed from

$$C_{ann} = C_{ann,cap.} + C_{ann,rep.} + C_{ann,O\&M} \tag{6}$$

In this study, the project lifetime is considered to be 25 years, and the current annual interest rate is 10%, while the inflation rate stands at 12%. These economic parameters are needed to compute the CRF. After that, HOMER uses the CRF to compute the NPC for various system configurations. HOMER aims to minimise the total net present cost (NPC) and cost of electricity (COE) by finding the optimal system configuration that matches the load demand and satisfies these constraints. It should be noted that all economic factors considered in HOMER are calculated in constant dollar (USD) terms.

Table 2. Economics and technical specification of various proposed system components [37].

S/N	Component	Parameter	Value	Unit
1.	Grid	Grid capital cost	0	$
		Import energy tariff	0.11	$/kWh
		Export energy tariff	0	$/kWh
2.	Solar PV	Capital cost	500	$/kW
		Replacement cost	450	$/kW
		Operation and maintenance cost	5	$/yr
		Lifetime	25	years
		Efficiency	20	%
		De-rating factor	88	%
		Temperature coefficient	−0.38	%/°C
3.	Wind turbine	Power output type	AC	
		Initial cost per unit	800	$/kW
		Replacement cost	700	$/kW
		Operation and maintenance cost	50	$/yr
		Hub height	24	m
		Lifetime	20	years
4.	Battery storage	Type	Lead–acid	
		Capacity	1	kWh
		Initial cost per unit	200	$
		Replacement cost	150	$
		Operation and maintenance cost	5	$/yr
		Maximum depth of discharge	20	%
		Throughput	800	kWh/yr

		Capital cost	300	$/kW
5.	Converter	Replacement cost	250	$/kW
		Operation and maintenance cost	5	$/yr
		Lifetime	15	year
		Inverter efficiency	95	%
		Rectifier efficiency	95	%
6.	Diesel generator	Initial cost per unit	195	$/kW
		Replacement cost	190	$/kW
		Operation and maintenance cost	0.03	$/h
		Lifetime	15,000	hours
		Conversion efficiency	30	%
		Diesel price	1.8	$/L
		Fuel curve slope	0.236	L/h/kW
7.	Control parameters	Project lifespan	25	year
		Simulation time step	1	hour
		Annual capacity shortage	0	%
		Expected Inflation rate	12	%
		Interest rate	10	%
		Dispatch strategy	Load following (LF)	

3.5. System Component Modelling for Hybrid Systems

3.5.1. PV Model

The power output of a photovoltaic cell is determined by several factors, including variation in solar radiation, module temperature, fill factor, shading, soiling, potential in-duced degradation and module orientation, and tilt angle. The most important factor here is solar radiation. The I–V characteristics of the solar cell change greatly with sunshine intensity S (W/m²) and cell temperature [40,41]. Figure 9 shows an equivalent circuit of the solar cell.
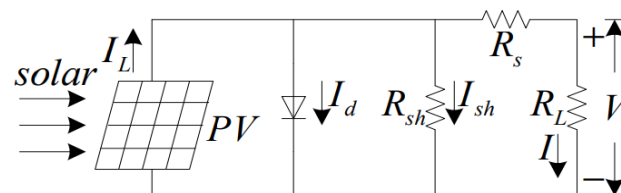

Figure 9. Equivalent circuit of the solar cell [42].

The corresponding I–V function is given as

$$I = I_L - I_o \left\{ exp \left[\frac{q(V + IR_s)}{AKT} \right] - 1 \right\} - \frac{V + IR_s}{R_{sh}} \tag{7}$$

$$V_{oc} = \frac{kT}{q} \ln \left(\frac{I_L}{I_o} + 1 \right) \approx \frac{kT}{q} \ln \left(\frac{I_L}{I_o} \right) \tag{8}$$

I = load current
I_L = photovoltaic current
I_o = reverse saturation current
q = electronic charge
k = Boltzmann constant
T = absolute temperature
A = factor of the diode quality

R_S = series resistance
R_{SH} = parallel resistance
V_{OC} = open circuit voltage

A group of PV cells constitute a module; some modules are arranged in series or parallel, and referred to as an array. Thus, the power of the PV array depends on the number of PV cells and modules coupled together. HOMER computes the power of the array using Equation (9).

$$P_{PV} = Y_{pv} f_{pv} \left(\frac{\overline{G}_T}{\overline{G}_{T,STC}} \right) \left[1 + \alpha_p (T_{cell} - T_{c,STC}) \right] \tag{9}$$

where

Y_{PV} = the rated capacity of the PV array, meaning its power output under standard test conditions [kW];
fPV = the PV derating factor [%];
$\overline{G}_T$ = the solar radiation incident on the PV array in the current time step [kW/m²];
$\overline{G}_{T,STC}$ = the incident radiation at standard test conditions [1 kW/m²];
αP = the temperature coefficient of power [%/°C];
T_{cell} = the PV cell temperature in the current time step [°C];
$T_{c,STC}$ = the PV cell temperature under standard test conditions [25 °C];

3.5.2. Wind Model

Wind turbines generate electrical energy from the kinetic energy of moving air, which is wind. This is achieved by the rotary motion produced as the wind breezes through coupled blade-like fans attached to an alternator. The power output of a wind turbine is given in Equation (10).

$$P_m = \frac{1}{2} \rho A V^3 C_e \tag{10}$$

where *p*, *A*, *V* and C_e represent air density (kg/m³), the turbine's swept area (m²), wind speed (m/s), and the maximum power extraction efficiency of the wind generator, usually referred to as the Bertz limit, with a peak value of about 0.59, respectively [43,44].

The meteorological information on wind characteristics used in this study are detailed in Section 3.2.2. Since the relative peak energy demand of the PHCs is roughly 5 kW, the wind turbine size selected for this work is a generic 1 kW wind turbine with a hub height of about 24 m.

3.5.3. Diesel Generator

The most important parameter for the diesel generator model is the fuel curve slope unit, given as L/h/kW output. The second parameter is the cost of fuel, which at the time of carrying out this study, was 1.8 $/L. In the generator inputs options, when the fuel curve inputs are computed, HOMER draws the corresponding efficiency curve [32]. The fuel consumption of the diesel generator, C_{onsG} (l/h) is modelled as dependent on the output power [44] from Equation (11).

$$F_G = B_G \times P_{G-rated} + A_G \times P_{G-out} \tag{11}$$

where $P_{G\text{-}rated}$ (kW) is the nominal power, $P_{G\text{-}out}$ (kW) is the output power of the diesel generator, and A_G and B_G are the fuel curve slope and the fuel curve intercept, respectively, defined by the user (l/kWh). The fuel curve slope given in the simulation data is 0.236 L/h/kW.

3.5.4. Battery Energy Storage

This is a very important aspect of the HRES. The battery storage system helps store available energy during the day and supply it at night or when there is a shortage of available renewable energy resources (wind and solar) [45]. Again, it should be pointed out that the behaviour of the battery with respect to the state of charge, autonomous runtime, depth of discharge, and other characteristics solely depends on the dispatch strategy utilised. Whilst cycle charging focuses on using available excess energy to charge the batteries, load following focuses on meeting the immediate demand of the load regardless of the battery storage capacity.

There are a number of available battery technologies used in renewable energy systems, some of which include: lithium ion–lithium manganese oxide (LMO), lithium nickel manganese cobalt oxide (NMC), lithium nickel cobalt aluminium oxide (NCA), lithium iron phosphate (LFP); lead acid-flooded, valve-regulated lead-acid (VRLA); nickel–nickel cadmium (NiCd); flow-redox flow batteries (RFB), and hybrid flow batteries [46]. Lead-acid batteries were selected for this research. The model is a 1 kWh battery with a nominal voltage of 12 V and a maximum capacity of 83.4 Ah. It has a roundtrip efficiency of 80%, a maximum charge current of 16.7 A, and a maximum discharge current of 24.3 A.

The charging of batteries occurs whenever the available energy supplied completely satisfies the available demand; thus, the excess is used for charging. The battery charge capacity at any instant can be computed from Equations (12) and (13) [9].

$$C_B(t) = C_B(t-1).(1-\sigma) + \left[P_T(t) - \frac{P_L(t)}{\eta_{inv}} \right] \times \eta_{Batt} \tag{12}$$

$$P_T(t) = N_{pv}P_{pv} + N_{wt}N_{wt} \tag{13}$$

where

$P_L(t)$ = load demand;
σ = battery self–discharging rate;
η_{inv} = inverter efficiency;
η_{Batt} = inverter efficiency;
$P_T(t)$ = total power generated by the RE sources at time *t*;
P_{pv} = power output of PV panel;
P_{wt} = output power of the wind turbine;
N_{pv} and N_{wt} = number of PV modules and wind turbines, respectively.

There are several models used to predict the expected lifespan of batteries, which depend on the operation conditions, the charge/discharge regime and temperature [45]. The operational lifetime of the battery can be prolonged if *DOD* is set within the range (30–50)%, depending on the manufacturer's specifications [9]. The maximum amount of power the storage bank can discharge over a specific time is given by Equation (14).

$$P_{batt,dmax,kbm} = \frac{-kcQ_{max} + kQ_1e^{-k\Delta t} + Qkc(1 - e^{-k\Delta t})}{1 - e^{-k\Delta t} + c(K\Delta t - 1 + e^{-k\Delta t})} \tag{14}$$

where

Q_1 = available energy [kWh] in the storage component at the beginning of the time step;
Q = total amount of energy [kWh] in the storage component at the beginning of the
Q_{max} = total capacity [kWh] of the storage bank;
c = the storage capacity ratio [unitless];
k = the storage rate constant [h^{-1}];
Δt = the length of the time step [h].

3.6. Dispatch Control Strategies

During the normal daily operations of demand centres, the energy consumed at every instant is different. This results from different load consumption cultures among consumers, time of day, peak load consumption, and the behaviours of loads, especially inductive loads. Sometimes, the rate of change or increase in instantaneous energy demand is so sudden that spikes can be identified in the load demand curves of the centres. In normal conditions, the energy supply is sufficient to meet average energy use, but when these spikes occur, there tends to be a deficiency in the energy supply. In such instances, strategies must account for the deficiency of energy supplied while ensuring that the system operates in optimal conditions and that energy excesses are reduced. A dispatch control strategy helps solve this problem. They are predefined rules and algorithms that control generator and storage unit operations when insufficient renewable energy resources supply the load [18].

Some of the existing dispatch strategies adopted by systems include load following (LF), cycle charging (CC), and combined dispatch strategy (CD). LF algorithms check and ensure that the generator supply is sufficient to power the primary load demand without charging the battery storage; CC dispatch strategy sees to it that the generator is operated at full capacity and excess supply is used to charge the batteries. CD encompasses LF and CC, using a trained model for predicting load behaviour, as it takes into consideration the future load demand and net present load consumption, and decides whether battery charging should be achieved using a generator or a renewable supply should be adopted [18,24,25].

LF strategy has been identified to be cost-effective in locations with high renewable energy potential, while CC strategy has mostly shown to be suitable in areas with limited renewable resources. Furthermore, it was observed from our review of the literature that the dispatch approach adopted in most grid-connected hybrid renewable energy systems (HRESs) that the grid acts as a reliable backup capable of delivering or absorbing surplus energy [47–51].

One disadvantage of the LF control strategy is that when the net load is less than the optimum operating capacity of the diesel generator, it may lead to underutilisation of the generator. On the other hand, when it is predicted that renewable energy sources will not be available in the near future or when the net load is lower than the optimal operating power of the generator, it is cost-effective to charge the battery and simultaneously supply the net load. However, this strategy can lead to missed opportunities to absorb excess renewable energy using the battery later in the day when RES become available, since the battery may have already been charged with the generator. This can result in higher greenhouse gas emissions and increased operation and maintenance (O&M) costs. However, this kind of operation creates substantial issues for developing nations such as Nigeria, wherein grid electrical supply can be unreliable and there is no policy regarding selling excess energy back to the grid.

4. Results and Discussion

This section presents the results obtained from the simulation of the resources at the selected sites. The project lifespan is 25 years, and the data presented here will help researchers' further work on rural electrification, especially in remote places in Nigeria. The results discussed here are the optimum configurations for the six considered sites. An analysis of the pollution and emissions from the proposed configurations, the electrical summaries, percentage contributions, renewable energy penetration, and a comparative analysis of the outcomes of the various sites with insights on factors that determine and affect the choice of some configurations are presented herein.

4.1. Optimum System Configurations

The optimum system configurations for the locations under study in this paper are detailed in Table 3. The results obtained from simulations in the HOMER Pro software with information on the components in the system configuration present for each configuration the respective sizing and economic data covering initial capital, net present cost (NPC), and cost of energy (COE). Systems involving diesel generators (DG) have further information on annual fuel consumption. The dispatch strategy adopted in the optimised solutions is the load-following dispatch strategy. An inflation rate of 12% is considered for the estimated lifespan of the project configuration of 25 years.

Based on these results, the best system configuration for all the sites considered is a hybrid PV/wind/diesel/battery/grid system, as shown in Table 3. The optimal configuration obtained for Kadassaka has the lowest NPC ($32,167) and COE (0.0667 $/kWh) of all the sites considered, followed by the Damare-polo site, with a $54,012 NPC and 0.0874 $/kWh COE. The low NPC and COE obtained from these sites are due to the sites' high availability of solar and wind resources compared to other sites.

Additionally, it was noted from the obtained results that one of the variables in determining the size (in kW) of the systems put together to power the site is the load demand of each site. HOMER chooses systems with lower ratings for locations with minimal energy demand and vice versa. Kadasaka is a station situated in an area with favourable wind patterns and dependable solar radiation levels. Although the Kadasaka PHC has a low energy requirement, HOMER chooses just the right number of PV and wind kilowatts to meet the demand, bringing the renewable fraction to 93.5%. As a result, these findings need to be cautiously interpreted while considering the potential for renewable sources and the highest possible demand.

Furthermore, compared with each site's present load profile and demand, the optimal and best system configuration allows for future load growth, as depicted in Figure 10. For instance, Doso, with a total present load power description of 9.7 kW, has an installed capacity under the best configuration (PV/wind/diesel/battery/ grid) of 29.8 kW. Additionally, in terms of the reduction of emissions through renewable integration, the two-period moving average line computed and depicted in Figure 10 shows that the average renewable fraction is above 45%.

Since the conventional standalone diesel generator and grid are presently employed in the selected rural healthcare facilities, it is considered the base case simulation. It is selected to allow a comparison to be made regarding the total savings that can be made in terms of cost and emissions when renewable energy sources are included in the design and implementation of the hybrid power system. This configuration (diesel–grid system) is observed to be the worst configuration, with the highest NPC ($1,180,000) and COE (0.866 $/kWh). More so, it has the highest initial capital cost of $2145 (as observed in the Doso PHC) among other base system configurations. High fuel consumption due to long hours of generator operation, high demand, and the associated maintenance costs have led to this high NPC. It is also noted that the COE of a diesel–grid system is approximately fifteen times the optimal configuration at all the selected sites. This observation has demonstrated that the configuration with the lowest capital cost may not necessarily be the configuration with the lowest energy cost. Conversely, the diesel-only system configuration NPC costs 30 times more than the best optimal configuration at the entire site. Therefore, adding renewable energy sources (wind and solar PV) and batteries to the existing diesel–grid system at the selected sites is considered a good investment in fuel savings and emission reduction.

Finally, the outcome depicts how sites with high renewable energy penetration are massively more favoured in sufficient and reliable power generation via renewable energy sources than the less potential areas. This can be explained by the percentage renewable fraction, which is clearly defined in the result in Table 3.

Table 3. Optimised system configurations for selected sites.

PHCs	System Configuration	Components Size					Conv.	Economics			Fuel Consp (L/yr)	RF (%)	Total Grid Purchase (kWh)	Dispatched Strategy
		PV (kW)	Wind (kW)	Diesel (kW)	Total Installed (kW)	Batt. (no.)	(kW)	Initial Cap ($)	Total NPC ($)	COE ($/kWh)				
Damare-Polo	PV–Wind–Diesel–Battery–Grid	5.5	4	4.4	13.9	58	3.86	19,565	54,012	0.0874	0.506	95.8	470	LF
	PV–Wind–Battery–Grid	5.35	4	—	9.35	57	3.22	18,242	55,836	0.0903	—	95.8	470	LF
	Diesel–Grid	—	—	4.4	4.4	—	—	858	495,571	0.801	4177	—	2276	CC
Agbalaenyi	PV–Wind–Diesel–Battery–Grid	14.9	5	8.8	28.7	58	7.5	27,004	77,224	0.0754	11.3	88.1	2174	LF
	PV–Wind–Battery–Grid	18.5	5	—	23.5	57	7.1	26,773	81,198	0.793	—	88.6	2112	LF
	Diesel–Grid	—	—	8.8	8.8	—	—	1716	882,843	0.862	7136	—	6862	CC
Doso	PV–Wind–Diesel–Battery–Grid	11.8	7	11	29.8	61	9.08	28,564	79,835	0.0588	6.32	93.7	1533	LF
	PV–Wind–Battery–Grid	11.6	7	—	18.6	60	8.13	25,852	84,414	0.0622		93.7	1539	LF
	Diesel-Grid	—	—	11	11	—	—	2145	1.18 M	0.866	13,104	—	8349	CC
Kadassaka	PV–Wind–Diesel–Battery–Grid	7.09	2	7	16.09	28	5.57	13,780	32,167	0.0667	7.24	93.5	551	LF
	PV–Wind–Battery–Grid	7.28	2	—	9.28	29	5.38	12,653	35,169	0.0729		93.7	549	LF
	Diesel–Grid	—	—	7	7	—	—	1365	728,227	1.51	5513	—	2680	CC
Ejioku	PV–Wind–Diesel–Battery–Grid	16.4	3	6.2	25.6	24	4.74	18,034	54,515	0.0791	10.7	90.9	1109	LF
	PV–Wind–Battery–Grid	15.9	4	—	19.9	24	4.17	17,181	57,620	0.0836	0	91.9	1014	LF
	Diesel–Grid	—	—	6.2	6.2	—	—	1209	631,458	0.916	9269	—	4010.381	CC

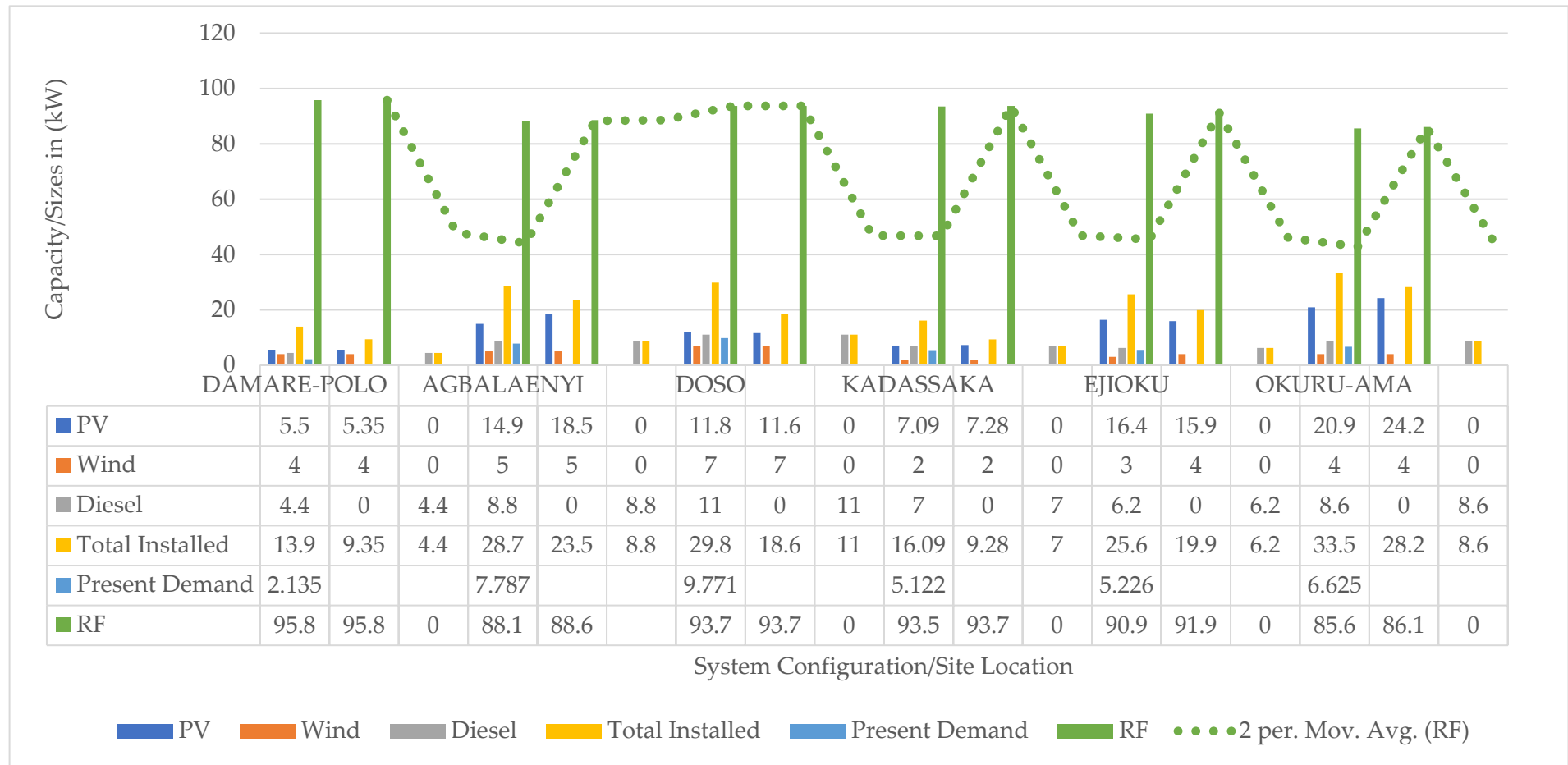|														
Okuru-Ama	PV–Wind–Diesel–Battery–Grid	20.9	4	8.6	33.5	72	7.53	31,981	114,903	0.115	18.8	85.6	2582	LF
	PV–Wind–Battery–Grid	24.2	4	—	28.2	72	7.3	31,896	118,820	0.119	—	86.1	2,21	LF
	Diesel–Grid	—	—	8.6	8.6	—	—	1677	850,331	0.847	6906	—	6451	CC

Figure 10. Comparative sizes of sources: installed capacity, present demand, and renewable fraction of installed power sources.

4.2. Electrical Energy Output of Optimum System Configuration

The summary of the optimum solutions is illustrated in Table 4. The data presented contain the results for PV, wind, diesel generator, and grid resources. Studies have shown that analysis of the yearly system performance of renewable energy resources suffices and provides ample information for decision making [52]. This results from the relatively similar behaviour or patterns of climatic data in terms of wind speed, irradiance from the sun, temperature, and other meteorological data. Hence, the data presented in this section are drawn from annual data and the system's behaviour.

Table 4. Summary of electrical energy output of optimum configuration.

Source	Metrics	Damare-Polo	Agbalaenyi	Doso	Ejioku	Kadasaka	Okuru-Ama
PV	Max. Output	5.85	15.9	12.4	17.7	7.58	22.2
	Total Annual Energy Production (kWh/yr)	9954	18,535	21,340	23,803	12,643	25,584
	% Contribution	38.1	49.3	37.8	74.2	59.4	74.9
Wind	Max. Output	4.0	5.0	7.0	3.0	2.0	4.0
	Total Annual Energy Production (kWh/yr)	15,689	16,891	33,599	7129	8075	5955
	% Contribution	60.1	44.9	59.5	22.2	37.9	17.4
D-Gen	Max. Output	1.10	2.98	2.75	1.55	1.75	2.15
	Total Annual Energy Production (kWh/yr)	1.10	25.0	13.8	23.3	15.8	40.9
	OPERATING HOUR (1 h/yr)	1.0	11	5	15	9	19
	% Contribution	0.0042	0.0664	0.0243	0.0725	0.074	0.12
Grid	Total Annual Energy Production (kWh/yr)	470	2174	1533	1109	551	2582
	% Contribution	1.80	5.78	2.71	3.46	2.59	7.56

4.3. Pollution and Emission Analysis

While analysing the potential of a hybrid renewable energy system, it is essential to consider the effect on the environment [35]. The HOMER Pro software evaluates the emission of six different pollutants. The pollutants include CO_2, CO, unburned hydrocarbon, particulate matter, SO_2, and NO. These pollutants are produced from generators or thermal boilers and are attributed to a negative environmental impact.

In this study, HOMER analysed the emission of each pollutant in kg/yr, whereby the proposed PV–wind–diesel–battery–grid system combinations contribute a very low emission rate compared to a base case of diesel–grid system for all the sites under study. Table 5 gives the comparative details of total emissions per year released into the environment.

Table 5. Comparative analysis of emission rate (kg/yr).

Configuration	Okuru-Ama	Kadassaka	Agbalaenyi	Damare-Polo	Dosso	Ejioku
Proposed system (kg/yr)	1692.28	369.54	23,325.35	12,545.13	991.499	733.9
Base case (kg/yr)	22,451.6	16,353	1413.32	299.94	30,828.28	16,232.90

5. Conclusions

This research paper vividly presents and discusses the adverse effects of electrical energy deficiency in residential and commercial sectors, focusing on Nigeria and the

affected public healthcare centres. We also highlighted Nigeria's available per capita energy, currently at 137.53 kWh per annum, which is technically insufficient and not sufficient meet the Sustainable Development Goal 7 (SDG 7) proposed by the United Nations. This energy shortage affects the general performance of PHCs in Nigeria, especially those in rural areas facing poor healthcare services and high mortality rates. In a bid to contribute positively to the stated problems, this paper looks into the situation of the power supply of the PHCs, and proffers solutions.

The areas selected for this research are spread across the six geographical zones in Nigeria, thus giving a broader insight into how systems configurations and optimal solutions for HRES are affected by their location and performance in the separate regions in Nigeria. These areas include Ejioku (Southwest), Kadassaka (Northwest), Damare Polo (Northeast), Doso (Northcentral), Agbalaenyi (Southeast) and Okuru-Ama (Southsouth) regions. The meteorological data sources for this report are very recent, being from as recent as 2020, and are from the Nigeria Meteorological Agency; this justifies our degree of confidence in said results, which form part of the optimisation parameters. The load profiles were collected on-site, and the techno-economic data are up to date, sourced from original equipment manufacturers and distribution companies' tariff rates in Nigeria. The results of this research will be useful and insightful in future works for providing grid-tied configurations to rural healthcare centres.

Author Contributions: Conceptualization, L.O.; Methodology, J.G.A.; Formal analysis, T.A.A.; Data curation, A.A.S.; Writing—review & editing, O.M.L. and K.E.J. All authors have read and agreed to the published version of the manuscript.

Appendix A

Table A1. Load analysis for Okuru-Ama, Agbalaenyi and Doso PHC.

PHC Centers	Okuru-Ama				Agbalaenyi				Dosso			
Load Description	Qty	Total Power (W)	Total on-Time (h/d)	Total Energy (kWh/d)	Qty	Total Power (W)	Total on-Time (h/d)	Total Energy (kWh/d)	Qty	Total Power (W)	Total on-Time (h/d)	Total Energy (kWh/d)
Multi-purpose refrigerators	1	330	18	5.94	1	330	18	5.94	2	660	16	10.56
Lab refrigerators	1	90	17	1.53	1	90	17	1.53	1	90	17	1.53
Surgical lights	2	18	4	0.072	2	18	4	0.072	2	18	4	0.072
Televisions	2	160	7.5	1.2	6	480	8	3.84	6	480	7	3.36
Ceiling fans	13	910	11	10.01	10	700	11	7.7	13	910	11	10.01
Water pumping machines	1	746	3	2.238	1	786	3	2.358	1	786	3	2.358
Lighting—indoor	27	405	9	3.645	17	255	9	2.295	20	300	12	3.6
Lighting—outdoor	14	560	12	6.72	13	520	12	6.24	15	600	12	7.2
Centrifuge	1	250	3	0.75	2	500	3	1.5	2	500	3	1.5
Haematology mixer	1	30	5	0.15	1	30	5	0.15	1	30	5	0.15
Haematology analyser	1	220	5	1.1	1	220	5	1.1	1	220	5	1.1
Desktop computer	1	160	6	0.96	1	160	6	0.96	2	320	6	1.92
Mobile charger	6	90	6	0.54	8	120	3	0.36	6	90	2	0.18
Vacuum aspirator	1	38	2	0.076	1	38	2	0.076	1	38	2	0.076

Load Description	Qty	Total Power (W)	Total on-Time (h/d)	Total Energy (kWh/d)	Qty	Total Power (W)	Total on-Time (h/d)	Total Energy (kWh/d)	Qty	Total Power (W)	Total on-Time (h/d)	Total Energy (kWh/d)
Oxygen concentrator	1	300	3	0.9	1	300	3	0.9	1	300	3	0.9
AC	2	2238	6	13.428	2	2238	6	13.428	3	3357	6	20.142
Microscope	1	30	6	0.18	5	100	2	0.2	6	120	2	0.24
Printer	1	50	6	0.3	1	50	6	0.3	2	100	6	0.6
VCR	-	-	-	-	1	20	2	0.04	1	20	2	0.04
Ultrasound machine	-	-	-	-	1	800	2	1.6	1	800	2	1.6
Radio—standby	-	-	-	-	1	2	24	0.048	1	2	24	0.048
Radio–transmitting	-	-	-	-	1	30	4	0.12	1	30	4	0.12
TOTAL		6625	129.5	**49.739**		7787	155	**50.757**		9771	154	**67.306**

Table A2. Load analysis of Ejioku, Kadasaka, Damare-polo PHC.

PHC Centers	Ejioku				Kadassaka				Damare-polo			
Load Description	Qty	Total Power (W)	Total on-Time (h/d)	Total Energy (kWh/d)	Qty	Total Power (W)	Total on-Time (h/d)	Total Energy (kWh/d)	Qty	Total Power (W)	Total on-Time (h/d)	Total Energy (kWh/d)
Multi-purpose refrigerators	1	200	7	1.4	1	300	10	3	1	200	10	2
Lab refrigerators	1	80	11	0.88	1	60	18	1.08	1	90	10	0.9
Surgical lights	1	40	3	0.12	-	-	-	0	-	-	-	0
Television	2	200	10	2	1	80	6	0.48	1	80	10	0.8
Ceiling fans	12	840	13	10.92	7	420	8	3.36	8	560	10	5.6
Water Pumping machines	1	1119	3	3.357	-	-	-	0	-	-	-	0
Lighting—indoor	8	120	15	1.8	8	120	8	0.96	14	210	13	2.73
Lighting—outdoor	8	192	12	2.304	6	240	12	2.88	10	400	12	4.8
Centrifuge	1	245	5	1.225	1	242	3	0.726	-	-	-	0
Haematology mixer	-	-	-	0	1	28	4	0.112	1	30	4	0.12
Haematology analyser	1	230	3	0.69	1	230	4	0.92	1	220	2	0.44
Desktop computer	1	200	5	1	1	150	5	0.75	-	-	-	0
Mobile charger	10	200	9	1.8	4	80	6	0.48	11	165	10	1.65
Vacuum aspirator	1	40	3	0.12	1	40	2	0.08	-	-	-	0
Oxygen concentrator	1	300	3	0.9	1	270	2	0.54	-	-	-	0
Lab autoclave	-	-	-	0	1	1500	2	3	-	-	-	0
Microscope	2	60	4	0.24	2	40	6	0.24	1	30	4	0.12
Printer	1	50	4	0.2	-			0	-	-	-	0
VCR	-	-	-	0	1	20	4	0.08	-	-	-	0
Ultrasound machine	-	-	-	0	1	800	2	1.6	-	-	-	0
Standby	-	-	-	0	1	2	24	0.048	-	-	-	0
Transmitting	-	-	-	0	1	30	4	0.12	-	-	-	0
Incubator	1	500	6	3	1	400	5	2	-	-	-	0
Hf radio transmitter	2	60	7	0.42	-	-	-	0	-	-	-	0
Electric sterilizer (autoclave)	1	100	3	0.3	-	-	-	0	1	150	2	0.3
Cd4 machine	1	200	4	0.8	-	-	-	0	-	-	-	0
X-ray machine	1	200	3	0.6	-	-	-	0	-	-	-	0
Blood chemical analyser	1	50	2	0.1	-	-	-	0	-	-	-	0
Blood bank regulator	-	-	-	0	1	70	18	1.26	-	-	-	0
Suction apparatus	-	-	-	-	1	100	2	0.2	-	-	-	0
Air conditional	-	-	-	-	-	-	-	-	1	1119	10	11.19
TOTAL		5226	135	**34.176**		5122	153	**23.916**		2135	87	**30.65**

References

1. Volotkovskaya, Y.; Volotkovskaya, N.; Semenov, A.; Semkova, A.; Fedorov, O.; Vladimirov, O. Analysis of the global energy resource market. In *E3S Web of Conferences*; EDP Sciences: Les Ulis, France, 2020; Volume 178, p. 01058. https://doi.org/10.1051/e3sconf/202017801058.
2. *Defining Energy Access: 2020 Methodology—Analysis—IEA*; IEA: Paris, France, 2023.

3.　Moss, T.; Bazilian, M.; Blimpo, M.; Culver, L.; Kincer, J.; Mahadavan, M.; Modi, V.; Muhwezi, B.; Mutiso, R.; Sivaram, V.; et al. The Modern Energy Minimum: The case for a new global electricity consumption threshold. Available online: https://www.rockefellerfoundation.org/wp-content/uploads/2020/12/Modern-Energy-Minimum-Sept30.pdf (accessed on 25 June 2023).

4.　Küfeoğlu, S. SDG-7 Affordable and Clean Energy. In *Emerging Technologies: Value Creation for Sustainable Development*; Springer International Publishing: Cham, Switzerland, 2022; pp. 305–330. https://doi.org/10.1007/978-3-031-07127-0_9.

5.　Statista Research Department. *Global Electricity Consumption by Country 2019*; Statista: New York, NY, USA, 2023.

6.　Olatomiwa, L.; Sadiq, A.A.; Longe, O.M.; Ambafi, J.G.; Jack, K.E.; Abd'Azeez, T.A.; Adeniyi, S. An Overview of Energy Access Solutions for Rural Healthcare Facilities. *Energies* **2022**, *15*, 9554. https://doi.org/10.3390/en15249554.

7.　Akbas, B.; Kocaman, A.S.; Nock, D.; Trotter, P.A. Rural electrification: An overview of optimization methods. *Renew. Sustain. Energy Rev.* **2022**, *156*, 111935. https://doi.org/10.1016/j.rser.2021.111935.

8.　Ebong, E.; Ekpenyong, C.; Eteng, E. Resource Distribution and Economic Advancement of Rural Communities in Nigeria. *Int. J. Adv. Res. Public Policy Soc. Dev. Enterp. Stud.* **2017**, *2*, 26–35.

9.　Olatomiwa, L.; Blanchard, R.; Mekhilef, S.; Akinyele, D. Hybrid renewable energy supply for rural healthcare facilities: An approach to quality healthcare delivery. *Sustain. Energy Technol. Assess.* **2018**, *30*, 121–138. https://doi.org/10.1016/j.seta.2018.09.007.

10.　Lee, K.; Kum, D. The Impact of Energy Dispatch Strategy on Design Optimization of Hybrid Renewable Energy Systems. In Proceedings of the 2019 IEEE Milan PowerTech, Milan, Italy, 23–27 June 2019; pp. 1–6. https://doi.org/10.1109/PTC.2019.8810977.

11.　Eidiani, M. *Integration of Renewable Energy Sources*; Springer: Cham, Switerland, 2022; pp. 1–25. https://doi.org/10.1007/978-3-030-72322-4_41-1.

12.　Soto, E.A.; Hernandez-Guzman, A.; Vizcarrondo-Ortega, A.; McNealey, A.; Bosman, L.B. Solar Energy Implementation for Health-Care Facilities in Developing and Underdeveloped Countries: Overview, Opportunities, and Challenges. *Energies* **2022**, *15*, 8602. https://doi.org/10.3390/en15228602.

13.　Prados, M.-J.; Pallarès-Blanch, M.; García-Marín, R.; del Valle, C. Renewable Energy Plants and Business Models: A New Rural Development Perspective. *Energies* **2021**, *14*, 5438. https://doi.org/10.3390/en14175438.

14.　Oladigbolu, J.O.; Al-Turki, Y.A.; Olatomiwa, L. Comparative study and sensitivity analysis of a standalone hybrid energy system for electrification of rural healthcare facility in Nigeria. *Alex. Eng. J.* **2021**, *60*, 5547–5565. https://doi.org/10.1016/j.aej.2021.04.042.

15.　Barley, C.D.; Winn, C.B. Optimal dispatch strategy in remote hybrid power systems. *Sol. Energy* **1996**, *58*, 165–179. https://doi.org/10.1016/s0038-092x(96)00087-4.

16.　Sinha, S.; Chandel, S. Review of software tools for hybrid renewable energy systems. *Renew. Sustain. Energy Rev.* **2014**, *32*, 192–205. https://doi.org/10.1016/j.rser.2014.01.035.

17.　Abnavi, M.D.; Mohammadshafie, N.; Rosen, M.A.; Dabbaghian, A.; Fazelpour, F. Techno-economic feasibility analysis of stand-alone hybrid wind/photovoltaic/diesel/battery system for the electrification of remote rural areas: Case study Persian Gulf Coast-Iran. *Environ. Prog. Sustain. Energy* **2019**, *38*, 1–15. https://doi.org/10.1002/ep.13172.

18.　Shezan, S.A.; Ishraque, F.; Muyeen, S.M.; Abu-Siada, A.; Saidur, R.; Ali, M.; Rashid, M. Selection of the best dispatch strategy considering techno-economic and system stability analysis with optimal sizing. *Energy Strat. Rev.* **2022**, *43*, 100923. https://doi.org/10.1016/j.esr.2022.100923.

19.　Sharma, S.; Sood, Y.R.; Maheshwari, A. Technoeconomic Feasibility and Sensitivity Analysis of Off-Grid Hybrid Energy System. In *Machine Learning, Advances in Computing, Renewable Energy and Communication: Proceedings of MARC 2020*; Springer: Singapore, 2021; pp. 113–121. https://doi.org/10.1007/978-981-16-2354-7_11.

20.　Agajie, T.F.; Ali, A.; Fopah-Lele, A.; Amoussou, I.; Khan, B.; Velasco, C.L.R.; Tanyi, E. A Comprehensive Review on Techno-Economic Analysis and Energy Storage Systems. *Energies* **2023**, *16*, 642. https://doi.org/10.3390/en16020642.

21.　Amini, S.; Bahramara, S.; Golpîra, H.; Francois, B.; Soares, J. Techno-Economic Analysis of Renewable-Energy-Based Micro-Grids Considering Incentive Policies. *Energies* **2022**, *15*, 8285. https://doi.org/10.3390/en15218285.

22.　Yahiaoui, A.; Tlemçani, A. A comparison study of HRES for electrificaion of a rural city in Algeria. *Wind. Eng.* **2022**, *47*, 528–545. https://doi.org/10.1177/0309524x221133810.

23.　Zebra, E.I.C.; van der Windt, H.J.; Nhumaio, G.; Faaij, A.P. A review of hybrid renewable energy systems in mini-grids for off-grid electrification in developing countries. *Renew. Sustain. Energy Rev.* **2021**, *144*, 111036. https://doi.org/10.1016/j.rser.2021.111036.

24.　Murugaperumal, K.; Raj, P.A.D.V. Feasibility design and techno-economic analysis of hybrid renewable energy system for rural electrification. *Sol. Energy* **2019**, *188*, 1068–1083. https://doi.org/10.1016/j.solener.2019.07.008.

25.　Odou, O.D.T.; Bhandari, R.; Adamou, R. Hybrid off-grid renewable power system for sustainable rural electrification in Benin. *Renew. Energy* **2020**, *145*, 1266–1279. https://doi.org/10.1016/j.renene.2019.06.032.

26.　Kalpana, D.R.; NageshaRao, S.H.; Siddaiah, R.; Mala, R. Case study on demand side management-based cost optimized battery integrated hybrid renewable energy system for remote rural electrification. *Energy Storage* **2022**, *5*, e410. https://doi.org/10.1002/est2.410.

27.　Al-Najjar, H.; El-Khozondar, H.J.; Pfeifer, C.; Al Afif, R. Hybrid grid-tie electrification analysis of bio-shared renewable energy systems for domestic application. *Sustain. Cities Soc.* **2022**, *77*, 103538. https://doi.org/10.1016/j.scs.2021.103538.

28. Alhawsawi, E.Y.; Habbi, H.M.D.; Hawsawi, M.; Zohdy, M.A. Optimal Design and Operation of Hybrid Renewable Energy Systems for Oakland University. *Energies* **2023**, *16*, 5830. https://doi.org/10.3390/en16155830.

29. Khortsriwong, N.; Boonraksa, P.; Boonraksa, T.; Fangsuwannarak, T.; Boonsrirat, A.; Pinthurat, W.; Marungsri, B. Performance of Deep Learning Techniques for Forecasting PV Power Generation: A Case Study on a 1.5 MWp Floating PV Power Plant. *Energies* **2023**, *16*, 2119. https://doi.org/10.3390/en16052119.

30. Medina-Santana, A.A.; Cárdenas-Barrón, L.E. Optimal Design of Hybrid Renewable Energy Systems Considering Weather Forecasting Using Recurrent Neural Networks. *Energies* **2022**, *15*, 9045. https://doi.org/10.3390/en15239045.

31. HOMER. How HOMER Calculates the Radiation Incident on the PV Array. 2023. Available online: www.homerenergy.com (accessed on 1 May 2023).

32. Delgado, A.; Gertig, C.; Blesa, E.; Loza, A.; Hidalgo, C.; Ron, R. Evaluation of the variability of wind speed at different heights and its impact on the receiver efficiency of central receiver systems. In *AIP Conference Proceedings*; AIP Publishing: Melville, NY, USA, 2016; Volume 1734. https://doi.org/10.1063/1.4949063.

33. HOMER. Wind Resource Variation with Height. Available online: https://www.homerenergy.com/products/pro/docs/3.11/wind_resource_variation_with_height.html (accessed on 1 May 2023).

34. Alayan, S. Design of a PV-Diesel Hybrid System with Unreliable Grid Connection in Lebanon. Master's Thesis, Dalarna University, Falun, Sweden, 2016.

35. Yakub, A.O.; Same, N.N.; Owolabi, A.B.; Nsafon, B.E.K.; Suh, D.; Huh, J.-S. Optimizing the performance of hybrid renewable energy systems to accelerate a sustainable energy transition in Nigeria: A case study of a rural healthcare centre in Kano. *Energy Strat. Rev.* **2022**, *43*, 100906. https://doi.org/10.1016/j.esr.2022.100906.

36. Krishan, O.; Sathans Design and Techno-Economic Analysis of a HRES in a Rural Village. *Procedia Comput. Sci.* **2018**, *125*, 321–328. https://doi.org/10.1016/j.procs.2017.12.043.

37. Rahmawati, A.Y. Price Hunter. 2020. Available online: http://www.ngpricehunter.com/ (accessed on 12 July 2023).

38. Eko, Electricity Distribution Company (EKDC). Tarrif Plans. 2016. Available online: https://ekedp.com/tariff-plans (accessed on 1 December 2022).

39. HOMER. Net Present Cost. Available online: www.homerenergy.com (accessed on 1 May 2023).

40. Dincer, F.; Meral, M.E. Critical Factors that Affecting Efficiency of Solar Cells. *Smart Grid Renew. Energy* **2010**, *1*, 47–50. https://doi.org/10.4236/sgre.2010.11007.

41. Vidyanandan, K.V. An Overview of Factors Affecting the Performance of Solar PV Systems. *Energy Scan* **2017**, *27*, 216.

42. Ma, X.; Sun, Y.; Wu, J.; Liu, S. The research on the algorithm of maximum power point tracking in photo voltaic array of solar car. In Proceedings of the 2009 IEEE Vehicle Power and Propulsion Conference (VPPC), Dearborn, MI, USA, 7–11 September 2009; pp. 1379–1382. https://doi.org/10.1109/VPPC.2009.5289450.

43. Manyonge, A.; Manyala, R.; Onyango, F.; Shichika, J. Mathematical Modelling of Wind Turbine in a Wind Energy Conversion System: Power Coefficient Analysis. *Appl. Math. Sci.* **2012**, *6*, 4527–4536.

44. Johnson, G.L. Wind Turbine Power. In *Wind Energy Systems*; Prentice Hall: Manhattan, KS, USA, 2001; pp. 1–54.

45. Dufo-López, R.; Bernal-Agustín, J.L. Multi-objective design of PV–wind–diesel–hydrogen–battery systems. *Renew. Energy* **2008**, *33*, 2559–2572. https://doi.org/10.1016/j.renene.2008.02.027.

46. Sita-Kengue, K. Solar + Storage: Battery Types for Solar Systems—Elum Energy. Elum Energy. Available online: https://elum-energy.com/blog/solarstorage-battery-types-for-solar-systems/ (accessed on 1 June 2023).

47. Adetoro, S.A.; Olatomiwa, L.; Tsado, J.; Dauda, S.M. A comparative analysis of the performance of multiple meta-heuristic algorithms in sizing hybrid energy systems connected to an unreliable grid. *e-Prime—Adv. Electr. Eng. Electron. Energy* **2023**, *4*, 100140. https://doi.org/10.1016/j.prime.2023.100140.

48. Adetoro, S.A.; Olatomiwa, L.; Tsado, J.; Dauda, S.M. An Overview of Configurations and Dispatch Strategies in Hybrid Energy Systems. In Proceedings of the 2022 IEEE Nigeria 4th International Conference on Disruptive Technologies for Sustainable Development (NIGERCON), Abuja, Nigeria, 5–7 April 2022; pp. 1–5. https://doi.org/10.1109/NIGERCON54645.2022.9803082.

49. Beyene, Y.B.; Worku, G.B.; Tjernberg, L.B. On the design and optimization of distributed energy resources for sustainable grid-integrated microgrid in Ethiopia. *Int. J. Hydrog. Energy* **2023**, *48*, 30282–30298. https://doi.org/10.1016/j.ijhydene.2023.04.192.

50. Oladigbolu, J.O.; Ramli, M.A.M.; Al-Turki, Y.A. Techno-Economic and Sensitivity Analyses for an Optimal Hybrid Power System Which Is Adaptable and Effective for Rural Electrification: A Case Study of Nigeria. *Sustainability* **2019**, *11*, 4959.

51. Shezan, S.A.; Kamwa, I.; Ishraque, F.; Muyeen, S.M.; Hasan, K.N.; Saidur, R.; Rizvi, S.M.; Shafiullah; Al-Sulaiman, F.A. Evaluation of Different Optimization Techniques and Control Strategies of Hybrid Microgrid: A Review. *Energies* **2023**, *16*, 1792. https://doi.org/10.3390/en16041792.

52. Siddaiah, R.; Saini, R. A review on planning, configurations, modeling and optimization techniques of hybrid renewable energy systems for off grid applications. *Renew. Sustain. Energy Rev.* **2016**, *58*, 376–396. https://doi.org/10.1016/j.rser.2015.12.281.